

# W-band MIMO GB-SAR for Bridge

Subjects: [Transportation Science & Technology](#)

Contributor: Massimiliano Pieraccini

This is a fast MIMO-GBSAR (Multiple-Input Multiple-Output Ground-Based Synthetic Aperture Radar) operating in W-band (77 GHz). The radar can complete a scan in less than 8 s. Furthermore, as its overall dimension is smaller than 230 mm, it can be easily fixed to the head of a camera tripod, which makes its deployment in the field very easy, even by a single operator.

ground-based synthetic aperture radar

radar interferometry

radar remote sensing

synthetic aperture radar

W-band

## 1. Introduction

Bridges require testing before going into service and need to be periodically monitored during their operative life for evaluating possible damage. Both testing and monitoring can be performed by static and dynamic measurements. The static test of a bridge is carried out by loading the deck with a dead load of several tons, and dynamic measurements are aimed at evaluating the response of the bridge stimulated by dynamic loads such as mechanical impulses, vibrodynes, and vehicular traffic.

Interferometric radars can perform both tests <sup>[1]</sup> operating in the real-aperture modality <sup>[2][3][4]</sup> or synthetic aperture modality <sup>[5][6]</sup>. The latter is usually called GB-SAR (Ground-Based Synthetic Aperture Radar).

Drawbacks of the current GB-SAR systems for structural monitoring are the slow acquisition rate (up to 90 s), physical dimensions (2–3 m) and weight (50–100 kg), which could preclude installation in many operative scenarios.

In order to reduce the acquisition time, MIMO (Multiple-Input Multiple-Output) systems have been proposed for bridge monitoring <sup>[7][8]</sup> and for environmental monitoring <sup>[9][10]</sup>. The MIMO radar reduces the acquisition time but dramatically increases hardware cost and complexity.

A way to reduce the size of a GB-SAR is operating at a higher frequency; for example, in W-band (77 GHz) instead of Ku-band (17 GHz). Radars operating in W-band have been proposed for different applications, especially in the automotive field <sup>[11][12][13][14]</sup>. These radars are characterized by small dimensions (often they are installed inside the headlight of a car) and by a fast repetition rate (up to 1500 Hz).

The first interferometric ArcSAR (circular synthetic aperture) operating in W-band was presented in 2018 <sup>[15][16]</sup> by IDS Georadar, Pisa, Italy. This sensor, named HYDRA, operates at 77 GHz and performs a scan with a minimum time of 30 s. The sensor is able to co-register a radar image with a three-dimensional lidar scanner. The radar acquisition is projected on the 3D surface and the sensor can provide the displacement information of a 3D volume.

In this paper, the authors present a fast and small GB-SAR operating at 77 GHz based on a multiple MIMO radar. The MIMO antennas are positioned orthogonally with respect to the linear rail (or actuator) and the radar moves at constant speed along the guide. The azimuth resolution is provided by the movement along the linear rail, while the elevation resolution is provided by the MIMO architecture. The GB-SAR operates on-the-fly acquisition [20] for increasing the acquisition speed, reducing the blurring due to moving targets, and for increasing the duty cycle (the ratio between the total acquisition time and the repetition time during a measurement cycle). The radar is able to scan the scene in less than 8 s (which is the mechanic limit of the used actuator).

The main novelty of the proposed radar, with respect to the scientific literature (e.g., [16][15]) is the scan time of the order of a few seconds obtained by combining on-the-fly acquisition and MIMO architecture for elevation resolution. This feature opens many practical applications that are precluded by slower radar systems.

## 2. Controlled Scenario

In order to evaluate the performance of the GB-SAR, the radar was operated in a controlled scenario. During these tests, the azimuth and elevation resolutions, and the interferometric uncertainty, were experimentally measured.

A corner reflector was located in front of the radar at a distance of

. The radar and the target were at the same height above the ground. Then, the radar was back-tilted with an elevation angle of  $25^\circ$ , as shown in **Figure 1**. Using this method, the target appeared to be lower than the radar. A micrometric displacement stage was fixed to the corner reflector. The micrometric displacement stage allows us to move the target using a micrometric screw with high reliability.



**Figure 1.** GB-SAR setup during the measurement in the controlled scenario.

The radar image can be focused on the vertical or horizontal plane. We focused the radar image on a horizontal x-y plane (**Figure 2**) by fixing the altitude, and on a vertical z-y plane (**Figure 3**) by fixing the abscissa. The altitude and the abscissa correspond to the target position.

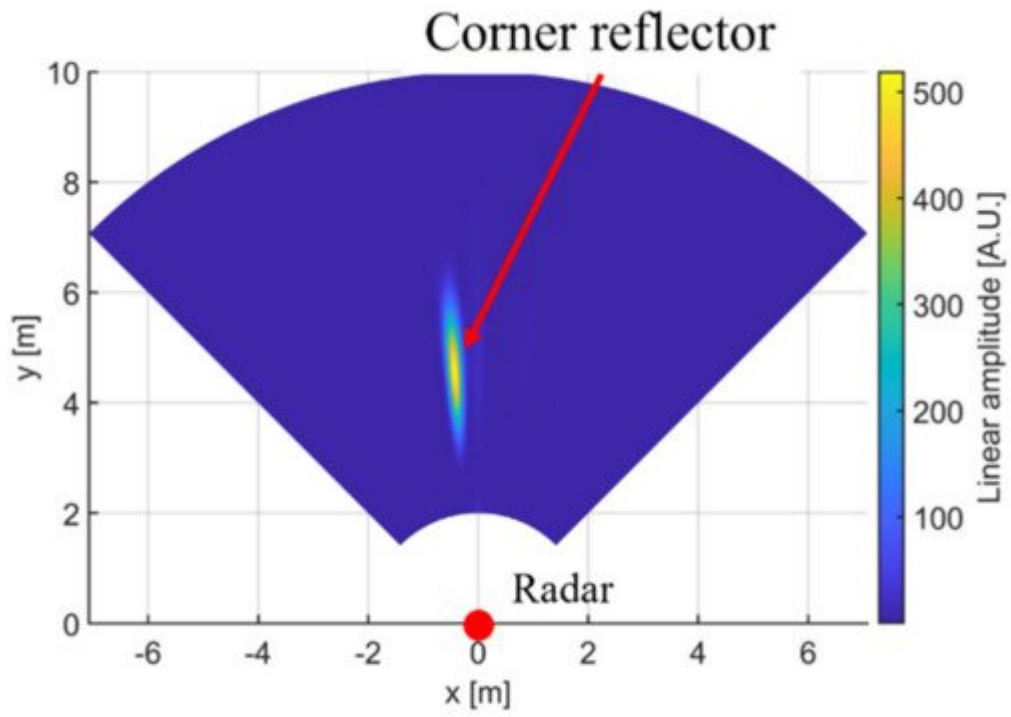
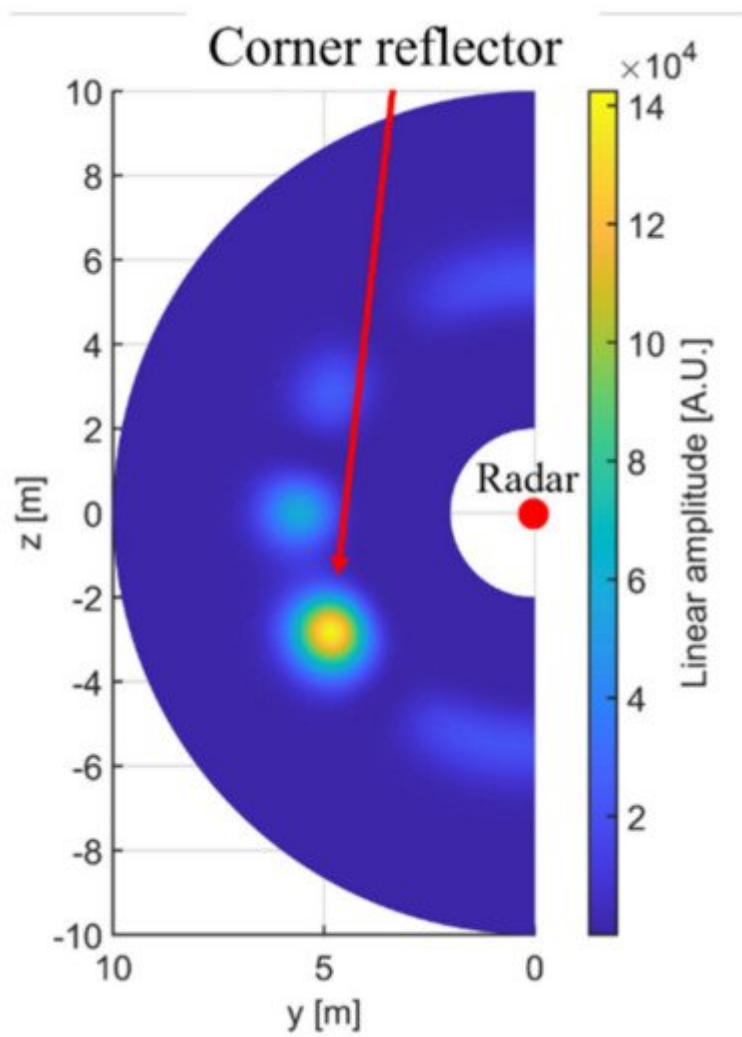


Figure 2. Radar image focused on the horizontal plane at



**Figure 3.** Radar image focused on the vertical plane at

**Figure 4** and **Figure 5** show the normalized point spread functions (PSF) at the range of the target in terms of azimuth and elevation.

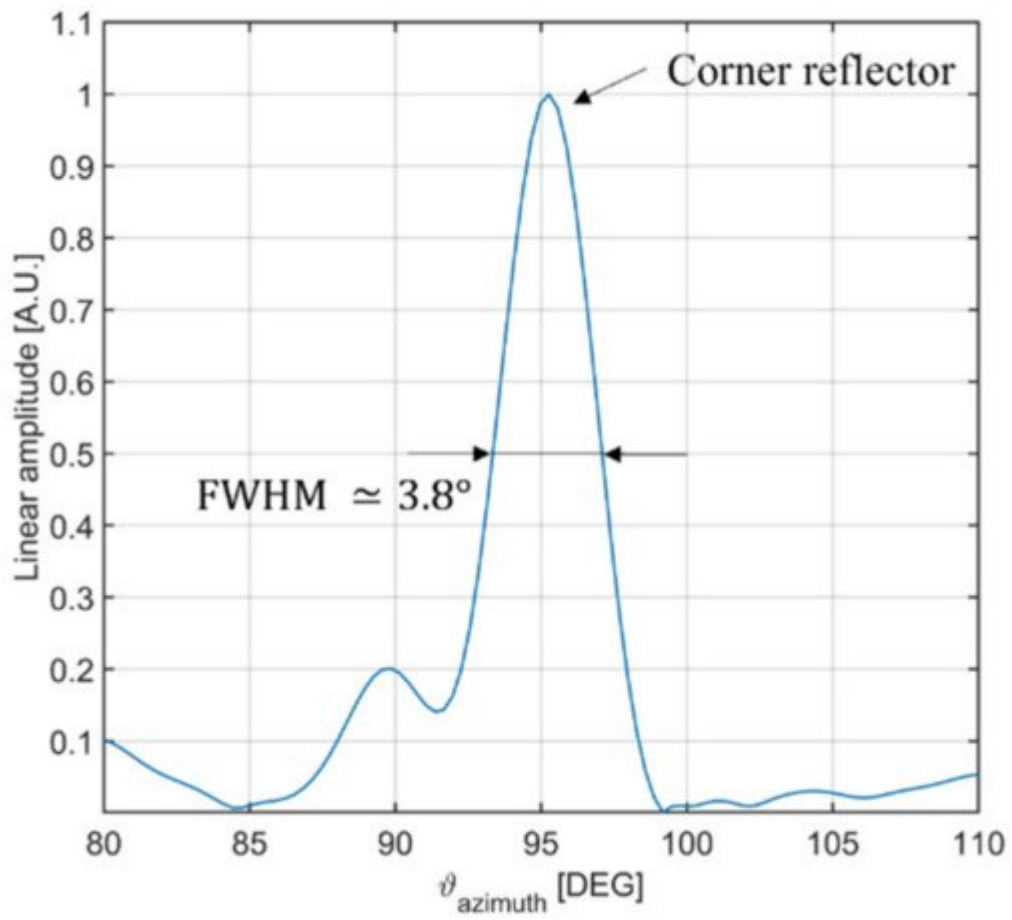
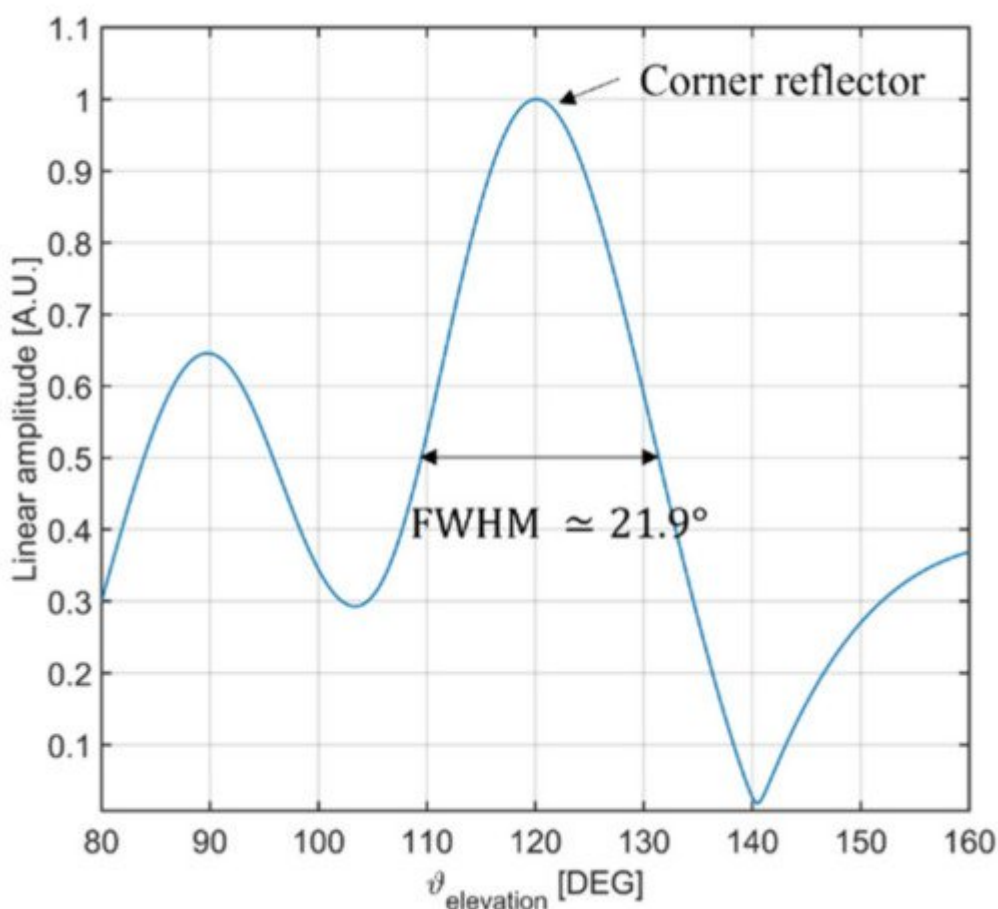


Figure 4. Point spread function in terms of azimuth.



**Figure 5.** Point spread function in terms of elevation.

The FWHM in azimuth was about  $3.8^\circ$  (**Figure 4**), and the FWHM in elevation was about  $22^\circ$  (**Figure 5**). Both values are in good agreement with theoretical values.

In order to verify the interferometric capability, the corner reflector was moved along the range direction with steps of 0.5 mm, towards the radar. The result of interferometric measurement is shown in **Figure 6**. The average displacement was \_\_\_\_\_ and the standard deviation 0.04 mm. These values are in good agreement with the current GB-SAR [27,28] (the measurement uncertainty of conventional GB-SAR is about 0.1 mm).

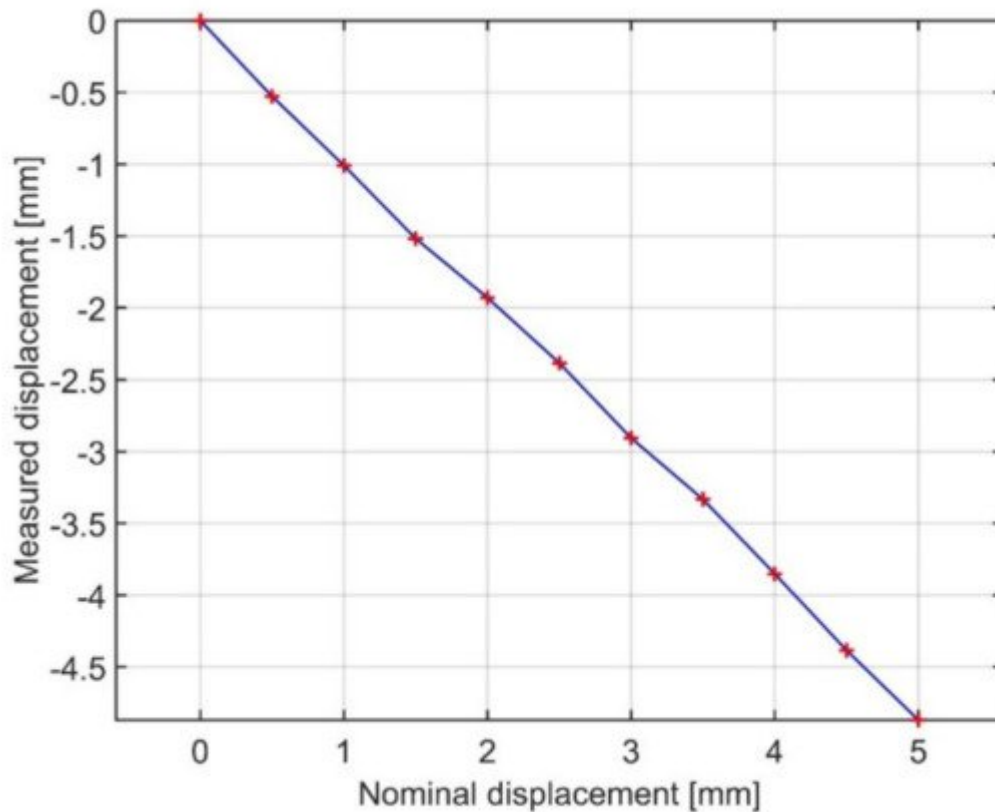


Figure 6. Displacement measured by GB-SAR in controlled scenario.

### 3. Vespucci Bridge, Florence, Italy

Static and a dynamic monitoring were performed on the Vespucci bridge in Florence, Italy. The bridge was designed and built between 1955 and 1957. The bridge is composed of three spans and two pillars. Since 2018, the bridge has been the object of a renovation and monitoring plan for consolidating the two pillars and the stalls inside the carriage [8].

The monitoring campaign, presented in this work, was interested in the central span, which is about 53 m long and 6.5 m in height. **Figure 7** shows the radar setup and the bridge span. The radar was located under the bridge, close to the right pillar of the central span in the middle of the carriage. The radar was back-tilted along the x-axis of about  $\alpha = 19^\circ$ . This value was considered during the focusing process. **Figure 14a** shows the reference system. The origin of the axis was in the middle of the radar scan. The x-y plan was leveled, so it can be considered on a horizontal plane. The z-axis was assumed to be vertical.



**Figure 7.** Radar setup (a) during the measurement campaign at Vespucci bridge (b).

The radar was at  
below the bridge and the left pillar was at about  
from the radar. The radar was exactly in the center of the roadway.

The focused image is shown in **Figure 7**. The echo was focused on a horizontal plane that corresponds to the bridge deck ( $z = 6.5$  m). The deck shape is well recognizable, and the signal from the pillar generated high side lobes.

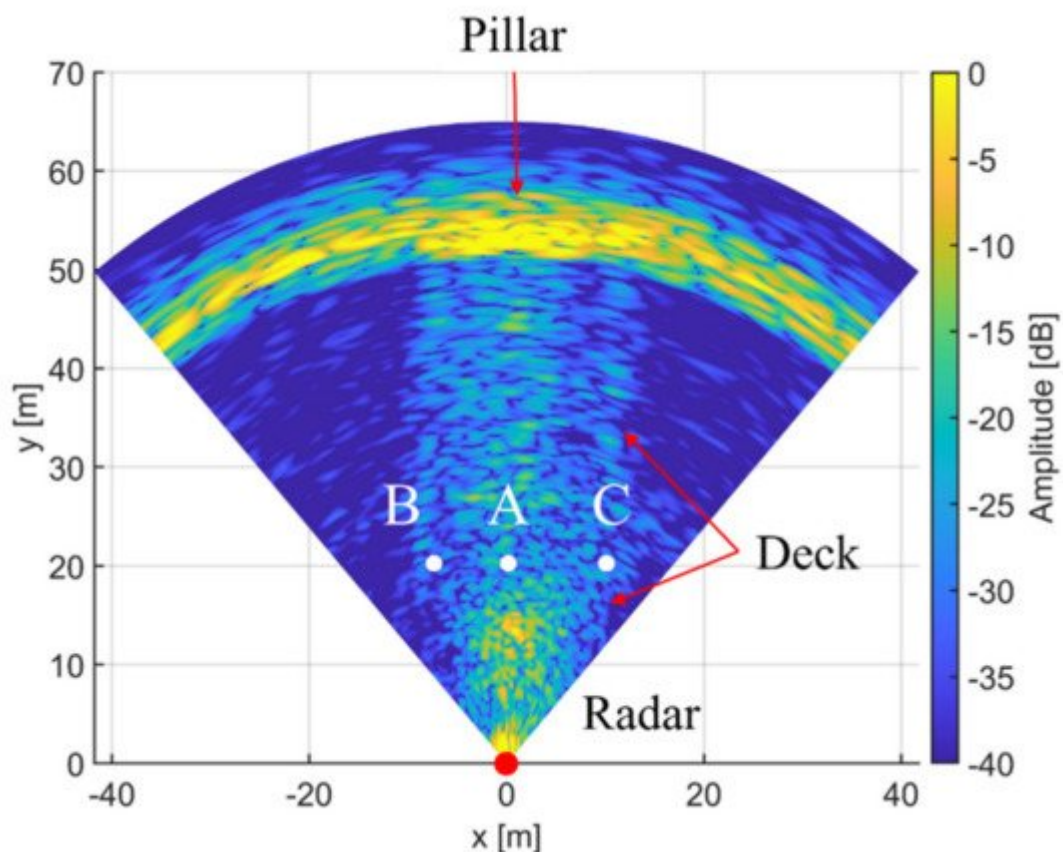


**Figure 7.** Radar image of Vespucci bridge focused on the horizontal plane at . The targets A, B, C were used for the displacement analysis.

The index of dispersion [29] image was calculated for discriminating the coherent pixels in the radar image (see **Figure 8**). Generally speaking, the dispersion index of a permanent scatterer has to be lower than 0.3. This value corresponds to the blue color in **Figure 8**. Most of the targets on the deck can be considered as permanent scatterers.

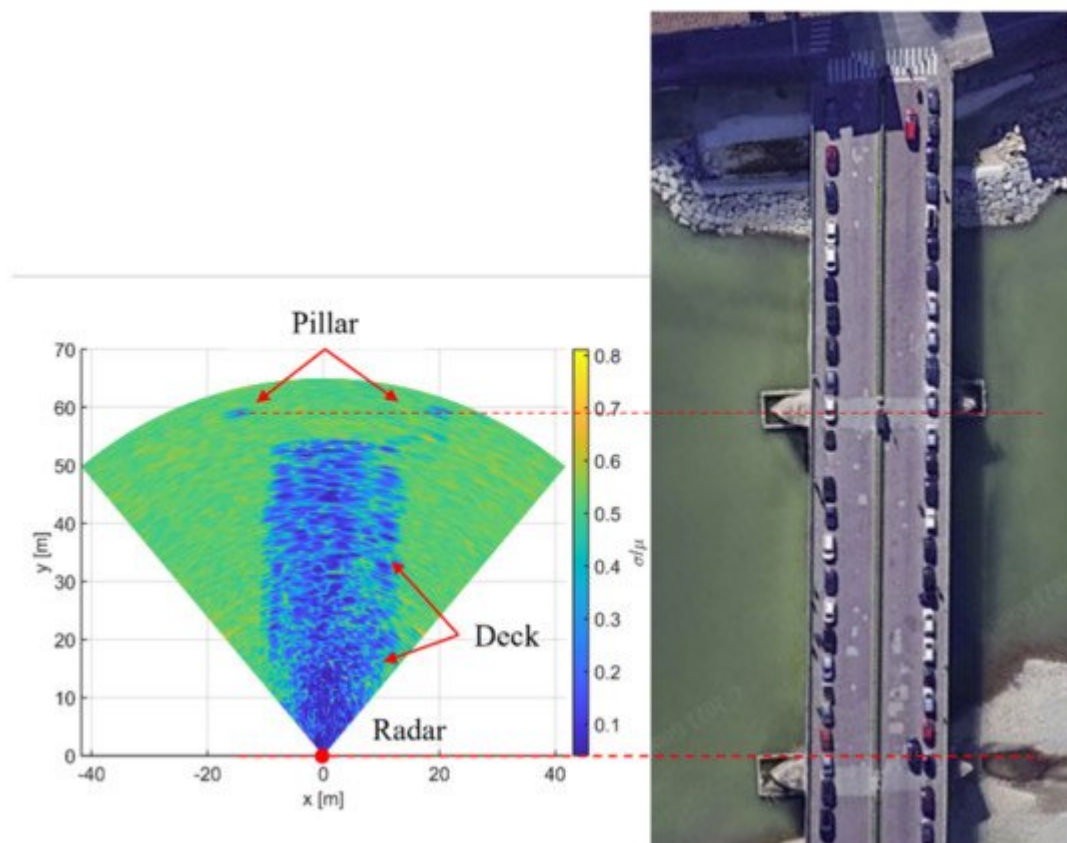


**Figure 16.** Index of dispersion of radar images of Vespucci bridge focused on the horizontal plane at

## 4. Conclusions

A fast interferometric MIMO GB-SAR operating at 77 GHz is proposed. The MIMO GB-SAR is based on a single-chip radar. The radar can acquire 3D images in less than 8 s with a theoretical azimuth resolution of  $1.75^\circ$  and an elevation resolution of  $10^\circ$ .

The system is also able to perform dynamic structural tests with an angular resolution of  $10^\circ$  and acquisition frequency up to 500 Hz.

The performance of the radar, in terms of angular resolution and interferometric capability, was preliminarily tested in a controlled environment.

Furthermore, the sensor was operated during a monitoring campaign on the historical Vespucci bridge in Florence, Italy. The MIMO GB-SAR was able to provide the displacement map on the deck surface with 0.125 Hz sampling frequency. Finally, operating in the only-MIMO modality, the radar was able to acquire the dynamic displacements of the deck stimulated by a truck crossing the bridge at speeds between 23 km/h and 50 km/h.

In conclusion, the fast MIMO GB-SAR proposed in this paper is able to perform both 3D GB-SAR acquisition in less than 8 s and dynamic measurement (at 500 Hz sampling frequency), even if with poor azimuth resolution. The proposed sensor is far from ready for industrialization, but it opens many practical applications precluded by slower and bulkier radar systems.

---

## References

1. Pieraccini, M.; Miccinesi, L. Ground-Based Radar Interferometry: A Bibliographic Review. *Remote Sens.* 2019, 11, 1029. [Google Scholar] [CrossRef]
2. Pieraccini, M. Monitoring of civil infrastructures by interferometric radar: A review. *Sci. World J.* 2013, 2013, 786961. [Google Scholar] [CrossRef] [PubMed]
3. Luzi, G.; Crosetto, M.; Fernández, E. Radar interferometry for monitoring the vibration characteristics of buildings and civil structures: Recent case studies in Spain. *Sensors* 2017, 17, 669. [Google Scholar] [CrossRef] [PubMed]
4. Shao, Z.; Zhang, X.; Li, Y.; Jiang, J. A comparative study on radar interferometry for vibrations monitoring on different types of bridges. *IEEE Access* 2018, 6, 29677–29684. [Google Scholar] [CrossRef]
5. Dei, D.; Mecatti, D.; Pieraccini, M. Static testing of a bridge using an interferometric radar: The case study of 'ponte degli alpini,' Belluno, Italy. *Sci. World J.* 2013, 2013, 7. [Google Scholar] [CrossRef] [PubMed]
6. Wang, Z.; Li, Z.; Mills, J. A new approach to selecting coherent pixels for ground-based SAR deformation monitoring. *ISPRS J. Photogramm. Remote. Sens.* 2018, 144, 412–422. [Google Scholar] [CrossRef]
7. Pieraccini, M.; Miccinesi, L. An Interferometric MIMO Radar for Bridge Monitoring. *IEEE Geosci. Remote. Sens. Lett.* 2019, 16, 1383–1387. [Google Scholar] [CrossRef]
8. Pieraccini, M.; Miccinesi, L.; Rojhani, N. Monitoring of Vespucci bridge in Florence, Italy using a fast real aperture radar and a MIMO radar. In *Proceedings of the IEEE International Geoscience and Remote Sensing Symposium, Yokohama, Japan, 28 July–2 August 2019*; pp. 1982–1985. [Google Scholar] [CrossRef]
9. Tarchi, D.; Oliveri, F.; Sammartino, P.F. MIMO Radar and Ground-Based SAR Imaging Systems: Equivalent Approaches for Remote Sensing. *IEEE Trans. Geosci. Remote. Sens.* 2013, 51, 425–

435. [Google Scholar] [CrossRef]
10. Hu, C.; Wang, J.; Tian, W.; Zeng, T.; Wang, R. Design and Imaging of Ground-Based Multiple-Input Multiple-Output Synthetic Aperture Radar (MIMO SAR) with Non-Collinear Arrays. *Sensors* 2017, 17, 598. [Google Scholar] [CrossRef] [PubMed]
  11. Cong, X.; Liu, J.; Long, K.; Liu, Y.; Zhu, R.; Wan, Q. Millimeter-wave spotlight circular synthetic aperture radar (scsar) imaging for Foreign Object Debris on airport runway. In Proceedings of the 12th International Conference on Signal Processing (ICSP), Hangzhou, China, 19–23 October 2014; pp. 1968–1972. [Google Scholar]
  12. Steiner, M.; Grebner, T.; Waldschmidt, C. Millimeter-Wave SAR-Imaging With Radar Networks Based on Radar Self-Localization. *IEEE Trans. Microw. Theory Tech.* 2020, 68, 4652–4661. [Google Scholar] [CrossRef]
  13. Hasch, J.; Topak, E.; Schnabel, R.; Zwick, T.; Weigel, R.; Waldschmidt, C. Millimeter-Wave Technology for Automotive Radar Sensors in the 77 GHz Frequency Band. *IEEE Trans. Microw. Theory Tech.* 2012, 60, 845–860. [Google Scholar] [CrossRef]
  14. Feger, R.; Haderer, A.; Stelzer, A. Experimental verification of a 77-GHz synthetic aperture radar system for automotive applications. In Proceedings of the 2017 IEEE MTT-S International Conference on Microwaves for Intelligent Mobility (ICMIM); Institute of Electrical and Electronics Engineers (IEEE), Nagoya, Japan, 19–21 March 2017; pp. 111–114. [Google Scholar]
  15. Daria, D.; Amoroso, G.; Bicci, A.; Coppi, F.; Cecchetti, M.; Rossi, M.; Falcone, P. Advanced tomographic tool for HYDRA radar system. In Proceedings of the 12th European Conference on Synthetic Aperture Radar, Aachen, Germany, 4–7 June 2018; pp. 1–3. [Google Scholar]
  16. Cecchetti, M.; Rossi, M.; Coppi, F. Performance evaluation of a new MMW Arc SAR system for underground deformation monitoring. In *Active and Passive Microwave Remote Sensing for Environmental Monitoring II*; SPIE: Bellingham, WA, USA, 2018; Volume 10788, p. 1078801.

---

Retrieved from <https://encyclopedia.pub/entry/history/show/36634>